

Synergistic Effect of Organo-Montmorillonite on Intumescent Flame Retardant Ethylene-Octene Copolymer

Jianbing Guo,¹ Min He,² Qingfeng Li,¹ Jie Yu,¹ Shuhao Qin¹

¹Division of technology R&D, National Engineering Research Center for Compounding and Modification of Polymer Materials, Guizhou, Guiyang 550014, China

²Research and Development Department (R&D), Guizhou Kumkuat Materials CO., LTD, Guizhou, Guiyang 550014, China

Correspondence to: S. Qin (E-mail: guojianbing_1015@126.com)

ABSTRACT: Nanocomposite of thermoplastic elastomer ethylene-octene copolymer/maleated ethylene-octene (POE/POE-g-MAH) with organo-montmorillonite (OMMT, 11 wt %) as masterbatch have been obtained by melt blending and it has been characterized by transmission electron microscopy (TEM). Flame retardant POE/POE-g-MAH/OMMT/ammonium polyphosphate-pentaerythritol (APP-PER) (an intumescent flame retardant with 75 wt % ammonium polyphosphate and 25 wt % pentaerythritol) composites were prepared by using melting processing to study their structures, flame-retardancy, thermal, and mechanical properties. TEM showed exfoliated structures throughout POE/POE-g-MAH/OMMT masterbatch and POE/POE-g-MAH/OMMT/APP-PER nanocomposites. Synergistic effect was observed between OMMT and APP-PER resulting in significant improvements on thermal stability, flame-retardancy and mechanical properties in the POE/POE-g-MAH/OMMT/APP-PER nanocomposites. © 2013 Wiley Periodicals, Inc. *J. Appl. Polym. Sci.* 129: 2063–2069, 2013

KEYWORDS: clay; elastomer; flame retardant; thermal properties; mechanical properties

Received 25 June 2012; accepted 9 December 2012; published online 7 January 2013

DOI: 10.1002/app.38920

INTRODUCTION

Polymers are versatile materials and used in a multitude of diverse areas. Although, physical and mechanical properties can be enhanced by fillers, but the lacking in flame-retardancy is the common problem of the polymers. In order to prevent combustion of the polymers, additives have been used. As is well known, the halogenated compounds are good flame-retardant additives, especially in synergistic combination with antimony trioxide. However, there are serious disadvantages such as the degradation products of halogenated compounds have environmental concerns associated with them.^{1–3} In the past few years, in the research to find halogen-free flame-retardant systems, intumescent flame-retardant (IFR) additives have found a place in polymer science as a method of providing flame-retardancy to polymers and they exhibit good efficiency.⁴ IFR is made up of three main additives, namely, an acid source, a carbonization agent and a blowing agent.^{5,6} Conventional IFR additives, which comprise ammonium polyphosphate (APP) in synergistic combination with pentaerythritol (PER) is good IFR additive. APP is the acid source and blowing agent, PER is the carbonization agent. APP-PER, while burning, gives a swollen multicellular char, which protects the underlying material from the action of the fire. The mechanism of this fire retardant is assumed that

the char acts as a physical barrier against heat transmission and oxygen diffusion, thus preventing pyrolysis of the materials to volatile combustible products.⁷ Although conventional APP/PER char has good intumescent properties, its physical and chemical properties and char layer structure need to be enhanced. Recent research into the application of organo-montmorillonite (OMMT) to conventional IFR additives has demonstrated that OMMT can improve the physical and chemical properties of char.⁸ Moreover, exudation and water solubility are problems associated with APP-PER. A migration of the mineral and exudation phenomena can occur when the samples are under air. Meanwhile, a large amount of APP-PER added to polymers will influence the other properties of polymers, in particular deteriorating the mechanical properties.^{9–12}

Nanocomposites have been attracted the interests of academics and industries in the past several decades due to their improved mechanical, thermal, flammability, ablation resistance, and enhanced barrier properties.¹³ Gilman et al.¹⁴ prepared nanocomposites of polymer and showed formation of intercalated composites with 25–39% reductions in peak heat release rate (PHRR) and equally significant reductions in mass loss rate (MLR) and average heat release rate for samples. Kazutoshi and HuanJun¹⁵ and Olaf et al.¹⁶ showed that the clay can

significantly improve the mechanical properties of the polymer. The synergistic effect between APP-PER and OMMT has been found including polypropylene,^{17,18} ethylene vinyl acetate⁷ and acrylonitrile-butadiene-styrene.¹⁹ Combinations of flame retardants may produce a synergistic effect of great importance for practical use.

The aim of this article is to investigate the synergistic effect of APP-PER and OMMT on the thermal properties, flame-retardancy and mechanical properties of POE/POE-g-MAH. Ethylene-octene elastomer (POE) has been widely used as the main polymer or a value enhancing ingredient in compound formulations. However, it seems that studies on thermal properties, flame-retardancy and mechanical properties of POE using the synergistic effect of APP-PER and OMMT are rare in our literature survey. To obtain a good dispersion of the organically modified clay in nonpolar POE, introduction of polymer functionalized with maleic anhydride (MAH) as a compatibilizer has been proved as a successful way to facilitate interactions between these two dissimilar components.^{13,20–22} In this article, to prepare the nanocomposites with a good dispersion of OMMT layers, we have designed and prepared POE/POE-g-MAH (20 wt %/ 80 wt %) with 11 wt % content of OMMT masterbatch. POE/POE-g-MAH/OMMT/APP-PER nanocomposites with different contents of POE/POE-g-MAH/OMMT masterbatch and APP-PER were prepared in a two-screw extruder and the synergistic effect of APP-PER and OMMT on the thermal properties, flame-retardancy and mechanical properties of POE/POE-g-MAH was discussed.

EXPERIMENTAL

Materials

The ethylene-octene elastomer (POE, Engage 8842, 45% octene, $M_w = 118,476$ and $M_n = 25,868$) was supplied by Dupont-Dow Chemicals. POE-g-MAH ($M_w = 112,921$ and $M_n = 24,758$, 45% octene) with a grafting degree of 0.6% was prepared by melt extrusion process. The intumescent flame retardant system contained APP ($n = 1000–2000$) was purchased from Presafer (Qingyuan) Phosphor Chemical Company and PER was provided by Tianjin Branch Close the Chemical Reagent. OMMT prepared from pristine Na^+ -MMT by ion exchange reaction using octadecylamine was provided by AMCOL International Co. Nanocor.

Preparation of Composites

Using dicumyl peroxide (DCP) as an initiator, the grafting reaction of POE with MAH was carried out by melt extrusion process. The POE-g-MAH with $\text{GD}(\%) = 0.6$ was prepared under $\text{MAH}(\%) = 1.0\%$, $\text{MAH}/\text{DCP} = 5$. The grafting chemistry of forming POE-g-MAH was prepared in a two-screw extruder (TSE-35A/400-44-22, $L/D = 35$, $D = 35$ mm, Coperion Keya Machinery, Nanjing, China) at $100–190^\circ\text{C}$ and the screw rotation speed was 170 rad/min and the feed speed was 1.6. OMMT was dried prior to use for 12 h at 80°C in a vacuum oven to remove any moisture. POE and POE-g-MAH were dried for 12 h at 50°C before use. POE/POE-g-MAH (20 wt %/80 wt %) with 11 wt % content of OMMT masterbatch and POE/POE-g-MAH/OMMT/APP-PER with different contents of POE/POE-g-MAH/OMMT masterbatch and APP-PER (Table I) were prepared in a two-screw extruder (TSE-35A/400-44-22, $L/D = 35$, $D = 35$ mm, Coperion

Table I. TG Data for POE/POE-g-MAH and Its Composites

Sample Code	$T_{5\%}$ ($^\circ\text{C}$)	W_{650} (%)
1#	351.51	0.61
2#	302.36	11.16
4#	308.35	12.94

$T_{5\%}$ is the temperature at 5% weight loss; W_{650} is the residue yield at 650°C .

Keya Machinery, Nanjing, China) at $110–180^\circ\text{C}$. The extrudates were pelletized and dried at 60°C for 24 h. The dried granules were compounded on a two-roll mill (Type SK-100, Shanghai Kechuang Rubber Plastic Mechanical Equipment, Shanghai, China) at 100°C for 3 min. The resulting composites were compression-moulded at 90°C for 5 min into standard samples.

Structural Characterization

Morphology was examined using transmission electron microscope (TEM, JEM 200CX, JEOL, Japan) at an accelerating voltage of 120 kV. Ultrathin sections (60–80 nm) were cut from Izod bars perpendicular to the flow direction under cryogenic conditions using a LKB-5 microtome (LKB, Switzerland).

TGA

The thermal properties of the composites were studied on TGA (TA, Q-50 Instruments) under 60 mL/min of compressed air and 40 mL/min flow of high purity grade nitrogen. About 8 mg each of the sample was loaded in a ceramic sample pan and heated from room temperature to 650°C at a heating rate of $20^\circ\text{C}/\text{min}$.

Limiting Oxygen Index

Limiting oxygen index (LOI) is the standard test method for measuring the minimum oxygen concentration to support candle-like combustion of plastics and was measured using a JF-3 type instrument (made by Jiang Ning Analytical Instrument Factory) on sheets $120 \times 6 \times 3 \text{ mm}^3$ according to the standard oxygen index test (ISO 4589: 2006).

UL-94 Test

The UL-94 vertically burning test was carried out using a SH5300 type instrument (made by HongKong Rehoboth Testing Equipment) on sheets (3-mm thick and 10-mm width) according to the standard of ISO 1210: 1996.

Cone Calorimeter

Flammability property of the samples ($100 \times 100 \times 6 \text{ mm}^3$) was carried out with an FTT, UK device according to ISO 5660 under a heat flux of $50 \text{ kW}/\text{m}^2$ at $20 \pm 2^\circ\text{C}$ and relative humidity $50 \pm 5\%$. The produced gases were collected in an exhaust duct system with centrifugal fan and the data were reported the average of three replicated experiments. The cone calorimeter data are the average of three measurements and the results are considered reproducible to $\pm 10\%$.

Mechanical Properties

Stress at 500% elongation and Unnicked Angle Tear Strength measurements were performed on a microcomputer control electronic universal testing machine (WdW210C type which was made by Shanghai Hualong Test Instrument) on sheets (2-mm thick) with a constant speed of 500 mm/min according to the

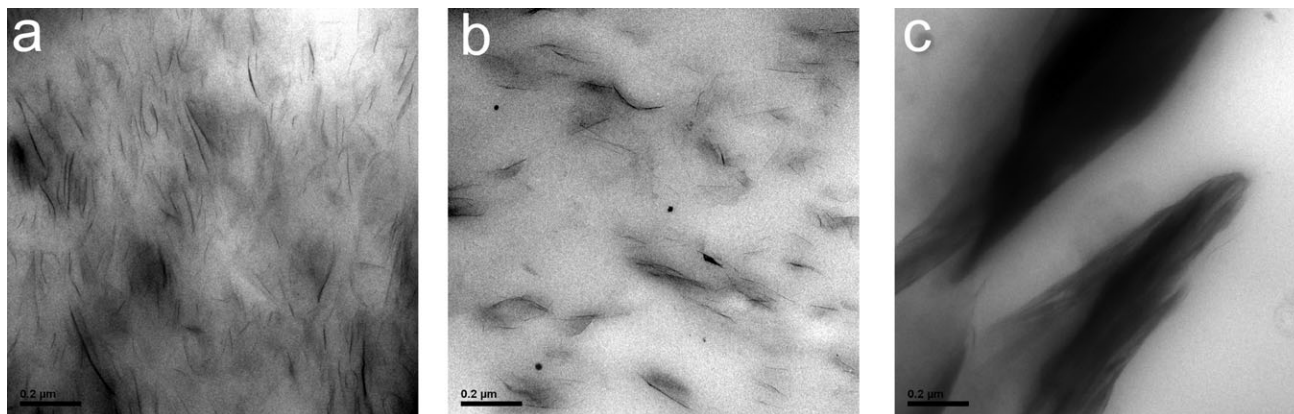


Figure 1. TEM microphotographs of composites; (a) POE/POE-g-MAH/OMMT (11 wt %) masterbatch, (b) POE-g-MAH/OMMT (3 wt %)/APP-PER (22 wt %) nanocomposite, (c) POE/OMMT (11 wt %).

Standard of ISO 37: 2005 and ISO 4589: 2006, respectively. The values are the average of 10 measurements and considered reproducible to $\pm 3\%$.

RESULTS AND DISCUSSION

Structural Characterization

Figure 1 shows TEM micrographs of POE/POE-g-MAH/OMMT (11 wt %) masterbatch, POE-g-MAH/OMMT (3 wt %)/APP-PER (22 wt %) nanocomposite and POE/OMMT (11 wt %) composite. Better dispersion of OMMT with many disordered single platelets is observed in both of the masterbatch [Figure 1(a)] and nanocomposite [Figure 1(b)], indicating delaminated mixed structures. Conversely, the OMMT layers consist of oriented multilayered stacks without intercalation or exfoliation occurred in POE/OMMT composite [Figure 1(c)].

The nonpolar POE lacks of favorable interactions with OMMT, which limits the dispersion of OMMT in POE during melt compounding. The polar character of MAH grafted on POE-g-MAH results in favorable interaction and thus a special affinity for the silicate surfaces. The strong hydrogen bonding between MAH groups of POE-g-MAH and the oxygen atoms of silicates leads to the increase of the interlayer spacing of the clay and the weakening of the interactions between the layers.²³

Thermal Properties

To exemplify the thermal behavior, the TG curves of POE/POE-g-MAH, POE/POE-g-MAH/APP-PER (25 wt %) and POE/POE-g-MAH/OMMT (2 wt %)/APP-PER (23 wt %) composites are shown in Figure 2. On heating the POE/POE-g-MAH decomposes within the temperature range of 250–550°C: The first stage (250–480°C) is attributed to the decomposition of POE and; the second step (480–550°C) corresponds to the degradation of cross-linked polymer made from the preparation of POE-g-MAH. The first step of weight loss for POE/POE-g-MAH/APP-PER (25 wt %) composite occurs in the range of 150–400°C due to the decomposition and esterification reaction between APP and PER; the second step of weight loss occurs within the temperature range of 400–480°C due to the degradation of the POE chains; the third step (480–650°C) corresponds

to the degradation of intumescent char. In the experiment, the POE/POE-g-MAH/OMMT (2 wt %)/APP-PER (22 wt %) nanocomposite shows the same degradation steps as POE/POE-g-MAH/APP-PER (25 wt %) composite.

The 5% mass loss temperature ($T_{5\%}$) and residue yield values at 650°C are summarized in Table I. $T_{5\%}$ of POE/POE-g-MAH/APP-PER (25 wt %) composite is lower than that POE/POE-g-MAH of due to earlier degradation of APP and PER. $T_{5\%}$ of POE/POE-g-MAH/OMMT (2 wt %)/APP-PER (23 wt %) is higher than that of POE/POE-g-MAH/APP-PER (25 wt %) composite due to the barrier effect of the better dispersion of OMMT, indicating that the OMMT improved to the thermal stability of the composites. The residue yield values at 650°C (W_{650}) for POE/POE-g-MAH/OMMT (2 wt %)/APP-PER (23 wt %) was 12.33% higher than that of POE/POE-g-MAH and 1.78% higher than that of POE/POE-g-MAH/APP-PER (25 wt %) composites.

Results from TG curves and the data show that the OMMT can enhance the thermal stability of flame retarded POE/POE-g-MAH/APP-PER composites and enhance the char formation.

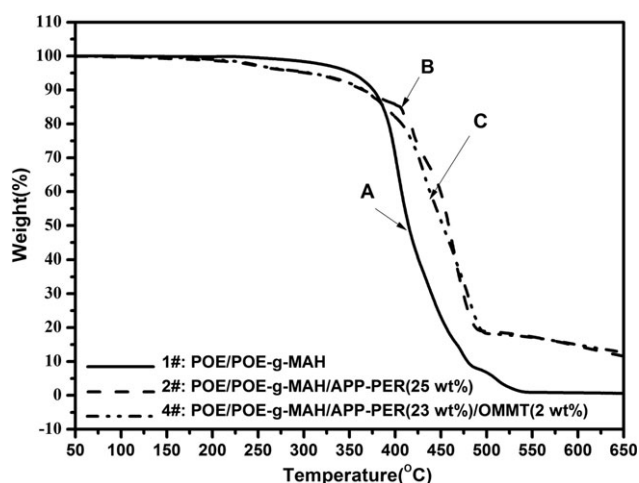


Figure 2. TG curves for POE/POE-g-MAH and its composites.

Table II. Results from LOI and UL-94 Data of POE/POE-g-MAH and Its Composites

	Sample code and formulation	LOI (%)	UL-94 test
1#	POE/POE-g-MAH	19.3	No rating, dripping
2#	POE/POE-g-MAH/APP-PER (25 wt %)	23.7	FV-0, no dripping
3#	POE/POE-g-MAH/OMMT(1 wt %)/APP-PER(24 wt %)	24.9	FV-0, no dripping
4#	POE/POE-g-MAH/OMMT (2 wt %)/APP-PER(23 wt %)	25.7	FV-0, no dripping
5#	POE/POE-g-MAH/OMMT (3 wt %)/APP-PER(22 wt %)	27.1	FV-0, no dripping

Flammability Properties

LOI and UL-94 tests are widely used to evaluate flame retardant properties of polymer.²⁴ LOI, which is a measure of flammability of the samples, is the minimum concentration of oxygen on oxygen/nitrogen mixture that will just support combustion.²⁵ The results for POE/POE-g-MAH and its composites are given in Table II. For POE/POE-g-MAH/OMMT/APP-PER nanocomposites, as OMMT increases, the flame-retardancy was improved, as reflected by the increased LOI value. For POE/POE-g-MAH/OMMT (3 wt %)/APP-PER (22 wt %) nanocomposite, the LOI value was 14.4% higher than the POE/POE-g-MAH/OMMT/APP-PER (25 wt %) composite and 40.4% higher than the POE/POE-g-MAH. The LOI tests indicate synergism between APP-PER and OMMT.

As can be seen from Table II, POE/POE-g-MAH had no rating with seriously dripping causing to ignite the absorbent cotton. POE/POE-g-MAH/APP-PER (25 wt %) composite passed the grade V-0 without dripping. With 1–3 wt % of OMMT the samples are able to pass the V-0 rating without dripping. It indicates that OMMT may cause the synergistic effect with APP-PER in the POE/POE-g-MAH/OMMT/APP-PER nanocomposites.

The cone calorimetric analysis can be conveniently used to measure not only heat release rates (HRR) but also many other flammability properties during burning,^{26,27} including time to ignition (TTI), PHRR, MLR, specific extinction area (SEA), smoke production rate (SPR) and so on. Cone calorimeter revealed improved flammability properties for many types of clay filled polymer nanocomposites. HRR, in particular peak HRR (PHRR) was found to be the most important parameter to evaluate fire safety.^{13,20,26,28–29}

HRR plots and cone calorimeter test data are shown in Figure 3 and Table III. TTI of POE/POE-g-MAH/APP-PER (25 wt %) is 9 s lower than POE/POE-g-MAH due to earlier degradation of APP and PER. For POE/POE-g-MAH/OMMT/APP-PER nanocomposites, TTI decreases with increasing OMMT loading, which could be ascribed to the low thermal stability of octadecylamine contained in the OMMT.³⁰ In the cone calorimeter test, the composites can be ignited easily as soon as the air and combustibles of thermal degradation products form the flammable mixture. The OMMT layers may cut off the heat at the composite surface to the substrate, making the heat assemble at the composite surface thus strengthening ignition.³¹

Just after ignition, the HRR of POE/POE-g-MAH composite increase more rapidly than those of its composites, reaching peaks of 1304 kW/m² at 347 s. For POE/POE-g-MAH/APP-

PER(25 wt %) composite, the time at PHRR is not retarded due to earlier degradation of APP-PER, both mean HRR and PHRR are decreased significantly. As OMMT increases, both the mean HRR and PHRR have further reduction. PHRR of POE/POE-g-MAH/OMMT (3 wt %)/APP-PER (22 wt %) nanocomposites display 84.4 and 51.9% reductions with respect to POE/POE-g-MAH and POE/POE-g-MAH/APP-PER (25 wt %) composite, respectively.

Figure 4 shows MLR curves for POE/POE-g-MAH and its composites. MLR of the flame retardant composites are lower than that of POE/POE-g-MAH, it increased in the following order: POE/POE-g-MAH > POE/POE-g-MAH/APP-PER (25 wt %) composite > POE/POE-g-MAH/OMMT (3 wt %)/APP-PER (22 wt %) nanocomposite. The MLR curves are in consistency with the HRR curves so that the reduction of MLR is primarily responsible for the lower HRR of the composites.

Figure 5 and Table III (Residue yield) shows that the residue yield of POE/POE-g-MAH/OMMT/APP-PER nanocomposites were strongly increased in comparison with POE/POE-g-MAH and POE/POE-g-MAH/APP-PER (25 wt %) composite. There is no residue yield was left for after combustion. The residue yield of POE/POE-g-MAH/APP-PER (25 wt %) is about 11.18%. As OMMT increased, the residue yield increased. The residue yield of POE/POE-g-MAH/OMMT (3 wt %)/APP-PER (22 wt %) is about 41.08%, displaying 267% increments comparison with POE/POE-g-MAH/APP-PER (25 wt %), respectively. Visual observations of the cone tests revealed that a char layer was formed and intumesced after the ignition of the material in the

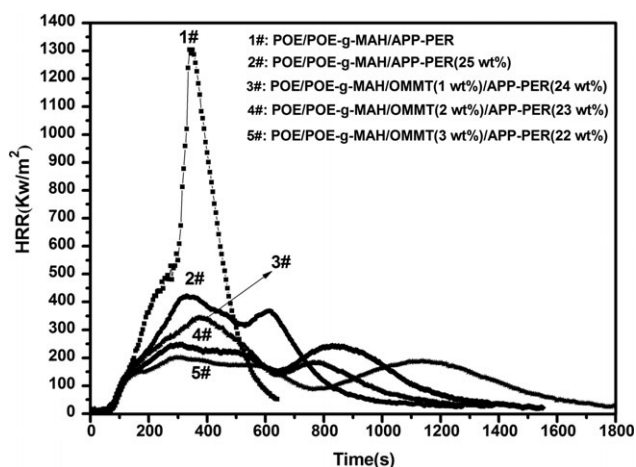
**Figure 3.** HRR curves for POE/POE-g-MAH and its composites.

Table III. Cone Calorimeter Test Data for POE/POE-g-MAH and Its Composites

Sample code	TTI(s)	Residue yield ($\pm 0.5\%$)	HRR (kw/m^2)		MLR (g/g)		Mean SEA (m^2/g)
			Peak	Mean	Peak	Mean	
1#	39	null	1304.12	422.10	0.088	0.319	328.49
2#	30	11.2	423.80	189.65	0.042	0.107	543.96
3#	29	18.4	344.55	152.36	0.039	0.089	551.71
4#	29	33.2	249.53	132.38	0.035	0.073	563.79
5#	27	41.1	203.47	125.95	0.028	0.068	579.74

case of POE/POE-g-MAH/APP-PER (25 wt %) and POE/POE-g-MAH/OMMT/APP-PER nanocomposites. It is to be noted that with OMMT the number of cracks formed during combustion was lower than that without OMMT. Moreover after combustion, the intumescent residue of the formulation containing OMMT seemed to be less fragile than that without OMMT. This tougher char can then reduce the fuel feeding the flame.

In general, APP (acid source and blowing agent) began to decompose at about 260°C , liberating phosphoric acid and large quantities of amine gas at the same time. The resulting acid triggered the first of a series of reactions starting with the dehydration of the carbonific compound and its subsequent charring. PER (carbonific) was dehydrated on acid attack through an esterification reaction at $320\text{--}360^\circ\text{C}$. The large quantities of amine gas from the decomposition of APP and the water vapor from the chemical reaction between phosphoric acid and PER caused the formation of a carbon-like foam layer over the substrate. An intumescent composition swelled up with the formation of a foam structure, which repelled the action of the fire until porous foam char layer was formed after system had fully cured and glued.^{8,32}

The study of Bourbigot et al.^{6,33} showed that the clay can react with APP to form aluminophosphates and the montmorillonite was completely collapsed by phosphate in solution. The aluminophosphates thermally stabilize the phosphorocarbonaceous structure. The aluminophosphate structure collapsed when the temperature increased leading to the degra-

ation of the phosphorocarbonaceous structure forming a ceramic-like structure. The ceramic-like structure can act as a protective barrier in addition to the intumescent shield and can limit the oxygen diffusion to the substrate and/or inhibit the migration of liquid or gaseous decomposition products into the hot zone. This barrier can hinder the formation of cracks. In the case of the composites without OMMT, no phosphorocarbonaceous structure was observed and, only a layer of orthophosphoric acid was observed in the intumescent char.

Finally, it is noteworthy that the appearance of APP-PER and OMMT increased the mean SEA (Table III). The SEA indicates the average value of the smoke evolved per mass unit of volatiles degraded from the sample upon burning. It is generally supposed that the volatile combustible products formed from the pyrolysis of polymer resin tend to leave the sample instantaneously. By leaving the polymer, these products cause the silicate to migrate to the sample surface and the clay layers become the dominant material, which might derive from the barrier effect for the diffusion of the volatile decomposition products to the gas phase as well as oxygen from the gas phase to the polymer.^{34,35} The released volatiles can not be burn enough due to the lack of exchange of oxygen leading to the increase of mean SEA. A char layer was formed and intumesced after the ignition of the material in the case of POE/POE-g-MAH/APP-PER (25 wt %) composite and POE/POE-g-MAH/OMMT/APP-PER nanocomposites, resulting in a higher mean SEA than that of POE/POE-g-MAH.

In this article, SPR indicates the danger of smoke production instead of SEA and is described as Formula (1). The SPR curves are shown in Figure 6.

$$SPR = MLR \times SEA \quad (1)$$

In Figure 6, the SPR of both the POE/POE-g-MAH/APP-PER (25 wt %) and POE/POE-g-MAH/OMMT/APP-PER composites are appreciably lower compared to POE/POE-g-MAH and decreased with the addition of the OMMT. Thus, the danger of smoke production is reduced with APP-PER and OMMT.

From the analysis of LOI, UL-94, and cone calorimeter tests, the synergistic effect can be observed between APP-PER and OMMT on the flame-retardancy.

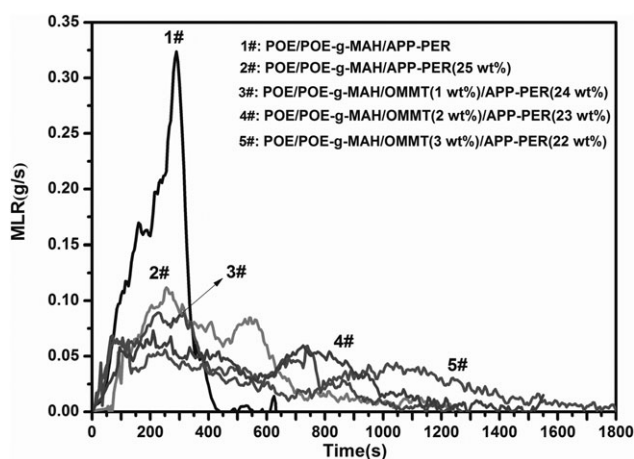


Figure 4. MLR curves for POE/POE-g-MAH and its composites.



Figure 5. Morphologies of the residues produced from the composites after cone calorimeter test. [Color figure can be viewed in the online issue, which is available at wileyonlinelibrary.com]

Mechanical Properties

Data for the stress at 500% elongation and unnicked angle tear strength of the POE/POE-g-MAH and its composites are presented in Table IV. Both stress at 500% elongation and unnicked angle tear strength of the POE/POE-g-MAH/APP-PER (25 wt %) composite are higher than those of POE/POE-g-MAH. The addition of OMMT increases the elongation and tear strength. It is to be noted here that the mechanical proper-

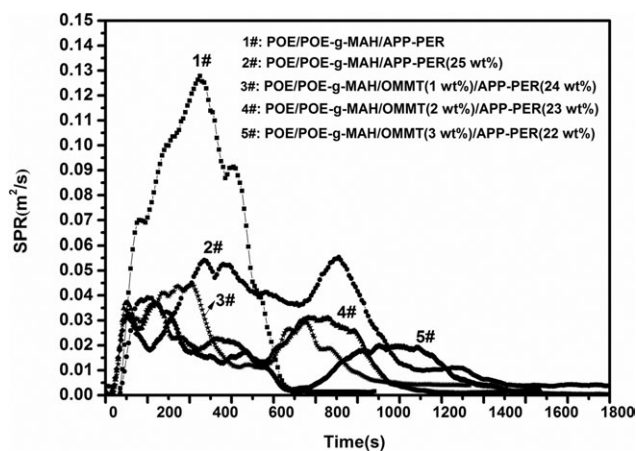


Figure 6. SPR curves for POE/POE-g-MAH and its composites.

Table IV. Mechanical Properties for POE/POE-g-MAH and Its Composites

Sample code and formulation	Stress at 500% elongation (MPa)	Unnicked angle tear strength (KN/m)
1# POE/POE-g-MAH	3.11	26.7
2# POE/POE-g-MAH/APP-PER (25 wt %)	3.96	33.2
3# POE/POE-g-MAH/OMMT (1 wt %)/APP-PER(24 wt %)	4.02	34.5
4# POE/POE-g-MAH/OMMT (2 wt %)/APP-PER(23 wt %)	4.45	36.1
5# POE/POE-g-MAH/OMMT (3 wt %)/APP-PER(22 wt %)	4.86	39.7

ties can be increased by both APP-PER and OMMT suggesting synergistic effect between APP-PER and OMMT. The OMMT is able to act as reinforcing filler due to its high aspect ratio and platelet structure.³⁶

CONCLUSION

TEM micrographs show exfoliated structures throughout POE/POE-g-MAH-/OMMT (11 wt %) masterbatch and POE/POE-g-MAH/OMMT/APP-PER nanocomposites. APP-PER has a good protection to POE chains. POE/POE-g-MAH/OMMT/APP-PER nanocomposites have better thermal stability than that of POE/POE-g-MAH/APP-PER due to the barrier effect of the better dispersion of OMMT, indicating that the OMMT improved to the thermal stability of the composites and enhance the char formation. LOI and UL-94 tests show that POE/POE-g-MAH/OMMT/APP-PER, as OMMT increases, the flame retardancy was improved, as reflected by the increased LOI value and passing the grade V-0 without dripping. Cone Calorimeter tests results show that TTI for both POE/POE-g-MAH/OMMT/APP-PER and POE/POE-g-MAH/OMMT/APP-PER nanocomposites are shorter compared to POE/POE-g-MAH matrix. HRR, MLR,

and SPR of the composites change significantly during the combustion tests in comparison with POE/POE-g-MAH matrix. From the analysis of LOI, UL-94 and cone calorimeter tests, the synergistic effect can be observed between APP-PER and OMMT on the flame-retardancy. The mechanical properties can be increased by both APP-PER and OMMT suggesting synergistic effect between APP-PER and OMMT.

ACKNOWLEDGMENTS

This work were supported by National Natural Science Foundation of China (20964001), National Natural Science Foundation of China (50863001), Project 973 (2011CB612313)

REFERENCES

1. Grace, C.; Panchatapa, J.; David, D. J.; Charles, A, W. *Polym. Degrad. Stab.* **2005**, *89*, 85.
2. Xie, F.; Wang, Y. Z.; Yang, B.; Liu, Y. *Macromol. Mater. Eng.* **2006**, *291*, 247.
3. Ebert, J.; Bahadir, M. *Environ. Int.* **2003**, *29*, 711.
4. Yun, L.; DeYi, W.; JunSheng, W.; YanPeng, S.; YuZhong, W. *Polym. Adv. Technol.* **2008**, *19*, 1566.
5. Xiaoping, H.; Weiyi, L.; Yuzhong, W. *J. Appl. Polym. Sci.* **2004**, *94*, 1556.
6. Bourbigot, S.; Le Bras, M.; Dabrowski, F.; Gilman J. W.; Kashiwagi, T. *Fire Mater.* **2000**, *24*, 201.
7. Yong, T.; Yuan, H.; Junfeng, X.; Jun, W.; Lei, S.; Weicheng, F. *Polym. Adv. Technol.* **2005**, *16*, 338.
8. Zhenyu, W.; Enhou, H.; Wei, K. *Prog. Org. Coat.* **2005**, *53*, 29.
9. Shinnjed, C.; Fengchih, C. *J. Appl. Polym. Sci.* **1999**, *72*, 109.
10. Sato, M.; Endo, S.; Araki, Y. *J. Appl. Polym. Sci.* **2000**, *78*, 1134
11. Zhao, C. S.; Huang, F. L.; Xiong, W. C.; Wang Y. Z. *Polym. Degrad. Stab.* **2008**, *93*, 1188.
12. Menachem, L. *Polym. Degrad. Stab.* **2005**, *88*, 13.
13. Ganesh, L.; Quentin, L.; Riko, O. *J. Mater. Sci.* **2008**, *43*, 2555.
14. Gilman, J. W.; Kashiwagi, T.; Nyden, M.; Brown, J. E, T.; Jackson, S.; Lomakin, S.; Giannelis, E. P.; Manias, E. Black-Well Scientific **1999**, p 249.
15. Kazutoshi, H.; HuanJun, L. *Macromolecules* **2006**, *39*, 1898.
16. Olaf, M.; Dirk, K.; Hans, W.; Christian, F.; Marc, V.; Holger, W. *Polymer* **2004**, *45*, 739.
17. Almeras, X.; Dabrowski, F.; Le Bras, M.; Poutch, F.; Bourbigot, S.; Marosi, G.; Anna, P. *Polym. Degrad. Stab.* **2002**, *77*, 305.
18. Haiyun, M.; Pingan, S.; Zhengping, F. *Sci. China Chem.* **2011**, *54*, 302.
19. Haiyun M.; Lifang T.; Zhongbin X. *Appl. Clay Sci.* **2008**, *42*, 238.
20. Huaili, Q.; Quansheng, S.; Shimin Z. *Polymer* **2003**, *44*, 7533.
21. Bourbigot, S.; Gilman, J. W.; Wilkie, C. A. K. *Polym. Degrad. Stab.* **2004**, *84*, 83.
22. Young, W. C.; Dongsuk, L.; Seong, Y. B. *Polym. Int.* **2006**, *55*, 84.
23. Hrissopoulou, K.; Anastasiadis, S. H. *Eur. Polym. J.* **2010**, *47*, 600.
24. Chuanmei, J.; Xilei, C. *Iran Polym. J.* **2009**, *18*, 725.
25. Kandola, B. K.; Horrocks, A. R.; Mylera, P.; Blairb, D. *Appl. Sci. Manufact.* **2002**, *33*, 808.
26. Yibing, C.; Fenglin, H.; Xin, X. *J. Mater. Eng. Perform.* **2010**, *19*, 171.
27. Haiyun, M.; Zhongbin, X.; Lifang, T. *Polym. Degrad. Stab.* **2006**, *91*, 2951.
28. Jeffrey, W. G. *Appl. Clay Sci.* **1999**, *15*, 31.
29. Zanetti, M.; Pierangiola, B.; Luigi, C. *Polym. Degrad. Stab.* **2004**, *85*, 657.
30. Xie, W.; Gao, Z.; Pan, WP.; Hunter, D.; Singh, A.; Vaia, R. *Chem. Mater.* **2001**, *13*, 2979.
31. Bo, L.; Lan, L.; Hongxin, L.; Yuanfang, L.; Demin, J. *Acta Polym. Sin.* **2007**, *5*, 458.
32. Duqusne, S.; Delobel, R. *Polym. Polym. Degrad. Stab.* **2002**, *77*, 333.
33. Bourbigot, S.; Le Bras, M.; Revel, B. *J. Mater. Sci.* **1999**, *34*, 5777
34. Tsu, H. C.; Wenjeng, G.; Kuo, C. C. *J. Polym. Res.* **2004**, *11*, 169.
35. Haiyun, M.; Lifang, T.; Zhongbin, X.; Zhengping, F. *Polym. Degrad. Stab.* **2007**, *92*, 1439.
36. HunSik, Kim.; Byung, H. P.; Jae, H. C.; JinSan, M. Y. *J. Appl. Polym. Sci.* **2008**, *107*, 2543.